

# Determination of the Gradient Flow Scale $t_0$ from a Mixed Action with Wilson Twisted Mass Valence Quarks

Alejandro Saez,<sup>a,\*</sup> Alessandro Conigli,<sup>a,b,c</sup> Julien Frison,<sup>d</sup> Gregorio Herdoíza<sup>a</sup> and Carlos Pena<sup>a</sup>

<sup>a</sup>*Department of Theoretical Physics, Universidad Autónoma de Madrid, 28049 Madrid, Spain  
and Instituto de Física Teórica UAM-CSIC, c/ Nicolás Cabrera 13-15  
Universidad Autónoma de Madrid, 28049 Madrid, Spain*

<sup>b</sup>*Helmholtz Institute Mainz, Johannes Gutenberg University, Mainz, Germany*

<sup>c</sup>*GSI Helmholtz Centre for Heavy Ion Research, Darmstadt, Germany*

<sup>d</sup>*ZPPT/NIC, DESY Zeuthen, Platanenallee 6, 15738 Zeuthen, Germany*

*E-mail:* [alejandro.saezg@uam.es](mailto:alejandro.saezg@uam.es)

We perform the scale setting procedure of a mixed action setup consisting of valence Wilson twisted mass fermions at maximal twist on CLS ensembles with  $N_f = 2 + 1$  flavours of  $O(a)$ -improved Wilson sea quarks. We determine the gradient flow scale  $t_0$  using pion and kaon masses and decay constants in the isospin symmetric limit of QCD as external physical input. We employ model variation techniques to explore the systematic uncertainties in the extraction of the ground state signal of lattice observables, as well as for the continuum-chiral extrapolations. We observe that the combined analysis of the mixed action data with that based on  $O(a)$ -improved Wilson valence quarks, provides an improved control of the extrapolation of  $t_0$  to the physical point.

*The 40th International Symposium on Lattice Field Theory (Lattice 2023)  
July 31st - August 4th, 2023  
Fermi National Accelerator Laboratory*

---

\*Speaker

## 1. Introduction

The validity of the Standard Model of particle physics has been verified in multiple ways over the years, through the consistency between its theoretical predictions and the corresponding experimental measurements. However, it is expected that the Standard Model is only an effective theory valid up to some energy scale. Searches for physical phenomena that deviate from its predictions are one of the main objectives in contemporary fundamental physics. One of the areas where New Physics is expected to appear is the quark-flavor sector of the Standard Model. A precise theoretical determination of the strong interaction effects is needed in order to reduce the theoretical uncertainties on flavour observables, and to uncover possible inconsistencies between theory and experiment. In this context, Lattice Field Theory is the key tool for calculating non-perturbative QCD contributions from first principles.

We consider a lattice setup [1–5] aimed to address the leading systematic uncertainties affecting charm-quark observables. It is based on a mixed-action regularisation consisting of Wilson twisted mass valence quarks combined with CLS ensembles with  $O(a)$ -improved Wilson sea quarks [11, 15]. Furthermore, the slowing down of the sampling of topological sectors at fine lattice spacings can be tamed by the use of open boundary conditions in the time direction [10].

A feature of this lattice regularisation is that when valence twisted mass fermions are tuned to maximal twist, an automatic  $O(a)$  improvement – up to residual mass effects from  $u, d, s$  sea quarks – can be achieved [2, 12]. This is of particular relevance when working with heavy quarks. In this work we present an update of the use of this lattice formulation in the light (up/down) and strange quark sectors. This is a necessary step before studying heavy quark physics, since a matching between the valence quark masses and the  $N_f = 2 + 1$  flavors in the sea is needed. Finally, we can carry out an independent computation of light-quark observables such as the pion and kaon decay constants and perform the scale setting using the gradient flow scale  $t_0$ .

## 2. Sea-quark sector: $O(a)$ -improved Wilson fermions

In the sea sector, we employ the set of CLS ensembles with open boundary conditions in the time direction collected in Table 1. They employ the Lüscher-Weisz gauge action with  $N_f = 2 + 1$  flavours of non-perturbatively  $O(a)$ -improved Wilson quarks.

These ensembles follow a chiral trajectory defined by a constant trace of the bare sea quark mass matrix

$$\text{Tr}(\mathbf{M}_q) = m_u + m_d + m_s = \text{constant}. \quad (1)$$

This ensures that the improved bare coupling  $\tilde{g}_0$  is kept constant up to  $O(a^2)$  effects when varying the quark masses at a fixed coupling  $\beta$ . However, since this condition is defined for the bare quark masses, we instead opt to follow a renormalised chiral trajectory by imposing that

$$\phi_4 = 8t_0 \left( m_K^2 + \frac{1}{2} m_\pi^2 \right) = 8t_0 m_K^2 + \frac{1}{2} \phi_2, \quad (2)$$

is kept fixed to its physical value. This choice corresponds at LO in  $\chi$ PT to fixing the sum of the renormalized quark masses, since

$$\phi_4 \propto m_u^R + m_d^R + m_s^R. \quad (3)$$

| $\beta$ | $a$ [fm] | id   | $m_\pi$ [MeV] | $m_K$ [MeV] |
|---------|----------|------|---------------|-------------|
| 3.40    | 0.086    | H101 | 420           | 420         |
|         |          | H102 | 350           | 440         |
|         |          | H105 | 280           | 460         |
| 3.46    | 0.076    | H400 | 420           | 420         |
| 3.55    | 0.064    | N202 | 420           | 420         |
|         |          | N203 | 340           | 440         |
|         |          | N200 | 280           | 460         |
|         |          | D200 | 200           | 480         |
| 3.70    | 0.050    | N300 | 420           | 420         |
|         |          | N302 | 340           | 440         |
|         |          | J303 | 260           | 470         |

**Table 1:**  $N_f = 2 + 1$  CLS ensembles [15] used in the sea sector. These ensembles employ non-perturbatively  $O(a)$ -improved Wilson fermions and open boundary conditions in the time direction.

The target chiral trajectory can be reached through a mass-shift of the simulated quark masses by Taylor expanding an observable  $O$  in the bare quark masses [16] as follows

$$\langle O(m'_u, m'_d, m'_s) \rangle = \langle O(m_u, m_d, m_s) \rangle + \sum_q (m'_q - m_q) \frac{d \langle O \rangle}{dm_q}. \quad (4)$$

Following [21], the sum in eq. (4) is restricted to  $q = s$  since shifting only the strange quark mass leads to an improved precision in the target observables. An educated guess for the physical value  $t_0^{\text{ph}}$ ,

$$\sqrt{t_0^{\text{iter}}} = 0.1445(6) \text{ fm}. \quad (5)$$

is selected as input of the final iteration leading to the value of  $\phi_4$  to which all observables are then mass-shifted. This specific value in eq. (5), is the outcome of the first steps of an *iterative* procedure starting from an initial guess of  $t_0$ , which is chosen free of uncertainties, and iterates the complete scale setting analysis, including correlations, until convergence to the value of  $t_0$  is reached. The steps of this procedure are illustrated in the right panel of Fig. 4. Using the isospin symmetric (isoQCD) values of the pion and kaon meson masses recommended in Ref. [25],

$$m_\pi^{\text{isoQCD}} = m_{\pi^0}^{\text{exp}} = 134.9768(5) \text{ MeV}, \quad (6)$$

$$m_K^{\text{isoQCD}} = m_{K^0}^{\text{exp}} = 497.611(13) \text{ MeV}, \quad (7)$$

leads to the value for  $\phi_4^* = 1.101(9)$ .

### 3. Valence-quark sector: Wilson twisted mass fermions

In the valence sector we use the Wilson twisted mass (Wtm) fermion action at maximal twist. This regularisation adds a chirally rotated mass term to the massless Wilson Dirac operator  $D_W$

including the Sheikholeslami-Wohlert term,

$$D_{\text{Wtm}} = D_{\text{W}} + m_0^{\text{val}} + i\gamma_5\mu_q^{\text{val}}, \quad (8)$$

where the  $m_0^{\text{val}}$  mass enters in the standard subtracted quark mass,  $m_q^{\text{val}} = m_0^{\text{val}} - m_{\text{cr}}$ , and  $\mu_q^{\text{val}}$  is the twisted mass parameter. Physical observables constructed from the Wtm Dirac operator are  $O(a)$ -improved – save for residual lattice artefacts of  $O(ag_0^4\text{Tr}(M_q))$  arising from sea quark masses – once the maximal twist condition is fixed by tuning the hopping parameter,  $\kappa^{\text{val}} = (2am_0^{\text{val}} + 8)^{-1}$ , so that the light ( $u, d$ ) valence PCAC quark mass vanishes,  $m_{12}^{\text{val}} = 0$ , on each ensemble.

#### 4. Matching sea and valence sectors

Since we are using a mixed action setup, to recover the unitarity of the theory in the continuum limit, we require the matching of the sea and valence quark masses. This matching can also be imposed in terms of the observables  $\phi_2, \phi_4$  defined in eq. (2), depending on the kaon and pion masses,

$$\phi_2^{\text{val}} \equiv \phi_2^{\text{sea}}, \quad \phi_4^{\text{val}} \equiv \phi_4^{\text{sea}}. \quad (9)$$

More specifically, we employ a set of measurements in the valence hyperplane ( $\kappa^{\text{val}}, a\mu_l^{\text{val}}, a\mu_s^{\text{val}}$ ) that allows to perform small interpolations to the valence parameters that satisfy eq. (9), in addition to simultaneously imposing the maximal twist condition,  $m_{12}^{\text{val}} = 0$ . The interpolation fit functions can be based on LO  $\chi$ PT. The matching procedure is illustrated in Fig. 1.

Having determined the valence *matching* parameters ( $\kappa^{\text{val},*}, a\mu_l^{\text{val},*}, a\mu_s^{\text{val},*}$ ) at which the maximal twist and the matching conditions in eq. (9) are simultaneously satisfied, it is then possible to also interpolate the valence pion and kaon decay constants to the same *matching* point.

We note that, throughout the analysis, finite volume effects are corrected using LO  $\chi$ PT [23]. These corrections are found to be smaller than the size of the statistical uncertainties for all observables and ensembles. The extraction of the ground state signal of lattice observables is based on a model variation over the Euclidean time fit intervals.

#### 5. Scale setting and determination of $t_0^{\text{ph}}$

The scale setting is carried out in terms of a linear combination of the pion and kaon decay constants in units of  $t_0$  [16],

$$\sqrt{8t_0}f_{\pi K} = \sqrt{8t_0} \times \frac{2}{3} \left( f_K + \frac{1}{2}f_\pi \right). \quad (10)$$

Up to logarithmic corrections, this quantity remains constant in SU(3)  $\chi$ PT at NLO along the renormalized chiral trajectory defined by  $\phi_4 \equiv \phi_4^*$ .

We will consider three sets of data in the scale setting analysis: (i) the *unitary* setup where the same  $O(a)$ -improved Wilson Dirac operator is used in the sea and valence sectors, which are referred to as the “Wilson” case; (ii) the mixed action setup after the matching procedure, referred to as “Wtm”; and (iii) the *Combined* set of data, in which the two previous sets are analysed simultaneously by imposing the universality of continuum-limit result. More specifically, the

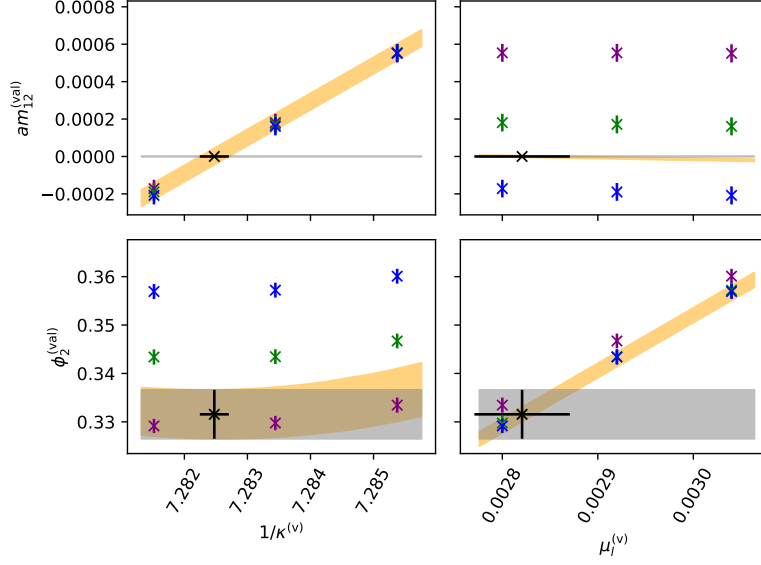


**Figure 1:** Top row: Light ( $u, d$ ) valence PCAC quark mass from the valence *grid* of points – in the hyperplane of input parameters  $(\kappa^{\text{val}}, a\mu_l^{\text{val}}, a\mu_s^{\text{val}})$  – interpolated to the maximal twist condition,  $m_{12}^{\text{val}} = 0$ . Bottom row:  $\phi_2^{\text{val}}$  along the valence grid, interpolated to the sea value  $\phi_2^{\text{sea}}$ . The sea sector parameters correspond to those of Table 1 for ensemble H105. The orange band in both figures represents the interpolation along the grid of valence parameters, while the horizontal grey line and band represent the target value to which we want to interpolate both observables. In the case of  $am_{12}^{\text{val}}$ , it is set to zero, and for  $\phi_2^{\text{val}}$  to  $\phi_2^{\text{sea}}$ . The interpolation of  $\phi_4^{\text{val}}$  is carried out in a similar way to that of  $\phi_2^{\text{val}}$ .

“Wilson” and “Wtm” data sets can be analysed independently, leading to two determinations of the physical value of  $t_0^{\text{ph}}$ . For the *Combined* case, a simultaneously fit of both data sets with independent sets of parameters characterising cutoff effects is performed. The lattice data can be parameterised as follows

$$\left(\sqrt{8t_0}f_{\pi K}\right)^{\text{latt}} = \left(\sqrt{8t_0}f_{\pi K}\right)^{\text{cont}} + c(a, \phi_2), \quad (11)$$

with  $c(a, \phi_2)$  a function describing cutoff effects. Several possible choices for the continuum behaviour and the cutoff effects are explored. For the continuum mass-dependence we consider SU(3)  $\chi$ PT expressions at NLO

$$\left(\sqrt{8t_0}f_{\pi K}\right)^{\text{cont}} = \frac{p_1}{8\pi\sqrt{2}} \left[ 1 - \frac{7}{6}L\left(\frac{\phi_2}{p_1^2}\right) - \frac{4}{3}L\left(\frac{\phi_4 - \phi_2/2}{p_1^2}\right) - \frac{1}{2}L\left(\frac{4\phi_4/3 - \phi_2}{p_1^2}\right) + p_2\phi_4 \right], \quad (12)$$

where,  $L(x) = x \log(x)$ . An alternative is to employ a Taylor expansion around the symmetric point  $\phi_2^{\text{sym}}$ ,

$$\left(\sqrt{8t_0}f_{\pi K}\right)^{\text{cont}} = p_1 + p_2(\phi_2 - \phi_2^{\text{sym}})^2. \quad (13)$$

To characterise the lattice spacing dependence, we consider

$$c(a, \phi_2) = c_1 \frac{a^2}{t_0} + c_2 \phi_2 \frac{a^2}{t_0} + c_3 \alpha_s^{\hat{\Gamma}} \frac{a^2}{t_0}, \quad (14)$$

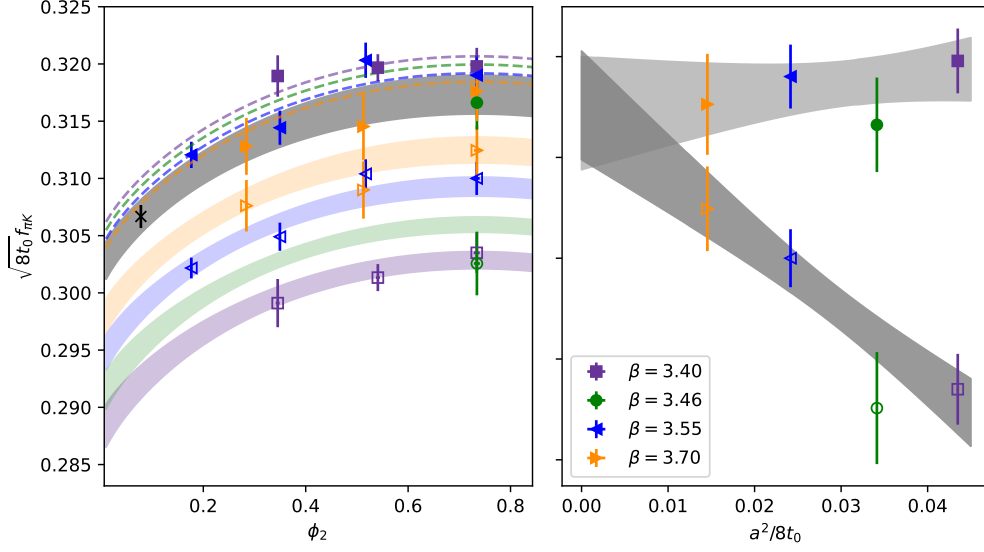


**Figure 2:** Left: Chiral and continuum extrapolations of  $\sqrt{8t_0}f_{\pi K}$ . We show the measurements for Wilson (empty points) and Wtm (filled points). The fit form in eq. (12) is used for mass dependence together with eq. (14) with  $c_2 = c_3 = 0$  to parameterise the lattice spacing dependence. No cuts are applied in this specific fit. Points with the same colour refer to a common value of the lattice spacing. The grey band represents the continuum limit dependence for the *Combined* data set analysis, while the coloured bands represent the chiral fits at each lattice spacing for the Wilson data, and, similarly, the dashed lines (without showing uncertainty in the fits) correspond to the Wtm case. Right: Continuum limit of symmetric point ensembles,  $m_\pi = m_K$ , with  $\phi_2 = 0.740(9)$ . A common continuum limit is not imposed in this fit.

and we examine the effect of switching on/off the different  $c_i$ 's. An exploratory study of the impact of including logarithmic corrections of  $O(a^2\alpha_s^{\hat{\Gamma}})$  considering the smallest value of the anomalous dimensions  $\hat{\Gamma}$  reported in [26] is also incorporated in the analysis by including the  $c_3$  term while setting  $c_1 = 0$ . We observe that the quality of the fit with cutoff effects of  $O(\phi_2 a^2)$  is poor for the current set of Wilson data, while a good description can be obtained for the Wtm data.

In addition to a variation of the functional forms, we explore the possibility of performing cuts in the data, by removing the coarsest lattice spacing  $\beta = 3.40$ , or by cutting the symmetric point ensembles with  $m_\pi = 420$  MeV.

The correlations present in the Monte Carlo data are retained throughout the analysis. In the chiral-continuum fit, the  $\chi^2$  function includes the correlations among the  $\sqrt{t_0}f_{\pi K}$  data points while the residual cross-correlations between  $\sqrt{t_0}f_{\pi K}$  and  $\phi_2$  are neglected in the fit. We observe, however, that this leads to a tiny deviation of the expectation value of the chi-squared [19],  $\langle\chi^2\rangle$ , away from the number of degree-of-freedom, i.e. the expected value when considering a correlated fit.

To study the systematic effects associated with model variation in the chiral and continuum extrapolations, we use the model averaging method introduced in [17] with the information criterion proposed in [18] to take into account fits that are not fully correlated. According to this information

criterion, each fit model is assigned a weight

$$W \propto \exp\left(-\frac{1}{2}\left(\chi^2 - \langle\chi^2\rangle\right)\right), \quad (15)$$

which allows to compute a weighted average for  $\sqrt{t_0}f_{\pi K}$  over the explored models. The method also assigns a systematic uncertainty coming from the model variation.<sup>1</sup> The model variation procedure and the corresponding model average are illustrated in Fig. 3. The specific model based on eq. (12) for the continuum behaviour and  $c_2 = c_3 = 0$  term in eq. (14) is shown in Fig. 2.

Once  $\sqrt{8t_0}f_{\pi K}$  is determined at the physical point (i.e. continuum limit result with physical pion and kaon masses), using a prescription for the isoQCD values of the pion and kaon decay constants [25]

$$f_{\pi}^{\text{isoQCD}} = 130.56(13) \text{ MeV}, \quad f_K^{\text{isoQCD}} = 157.2(5) \text{ MeV}, \quad (16)$$

as physical inputs, it is possible to determine the physical value of the gradient flow scale  $t_0^{\text{ph}}$ . Our results for the three types of analysis (Wilson, Wtm and Combined), together with a comparison with other studies also based on  $N_f = 2 + 1$  CLS ensembles, are presented in Fig. 4. We observe a shift of the central value of  $t_0$  with respect to the result of Bruno et al. [16] — which is based on a similar set of ensembles than the one employed in this work — depending on whether the physical inputs of FLAG21 [25] or FLAG16 [24] are considered.

## 6. Conclusions

We have presented an update of a scale setting procedure based on physical inputs for the pion and kaon decay constants, using a mixed action consisting of twisted mass valence quarks on CLS  $O(a)$ -improved sea quarks [27]. We have explored the systematic effects associated to model variation in the chiral and continuum limits, and demonstrated the effectiveness of combining the Wilson and mixed action (Wtm) calculations to improve the precision of  $t_0$ . In the near future we plan to extend this study by adding ensembles at finer lattice spacings and with physical pion masses, which will allow to consider an analysis where physical input from only the pion decay constant is employed in the determination of  $t_0$ . Furthermore, we plan to determine the light quark masses and to pursue our charm physics project based on this mixed action approach [7–9].

## Acknowledgements

We are grateful to our colleagues in the Coordinated Lattice Simulations (CLS) initiative for the generation of the gauge field configuration ensembles employed in this study. We acknowledge PRACE for awarding us access to MareNostrum at Barcelona Supercomputing Center (BSC), Spain and to HAWK at GCS@HLRS, Germany. The authors thankfully acknowledge the computer resources at MareNostrum and the technical support provided by Barcelona Supercomputing Center (FI-2020-3-0026). We thank CESGA for granting access to Finis Terrae II. This work is partially supported by grants PGC2018-094857-B-I00 and PID2021-127526NB-I00, funded by

<sup>1</sup>We have also considered this model averaging technique to extract the ground state signal of the relevant lattice observables by scanning over Euclidean-time fit intervals.

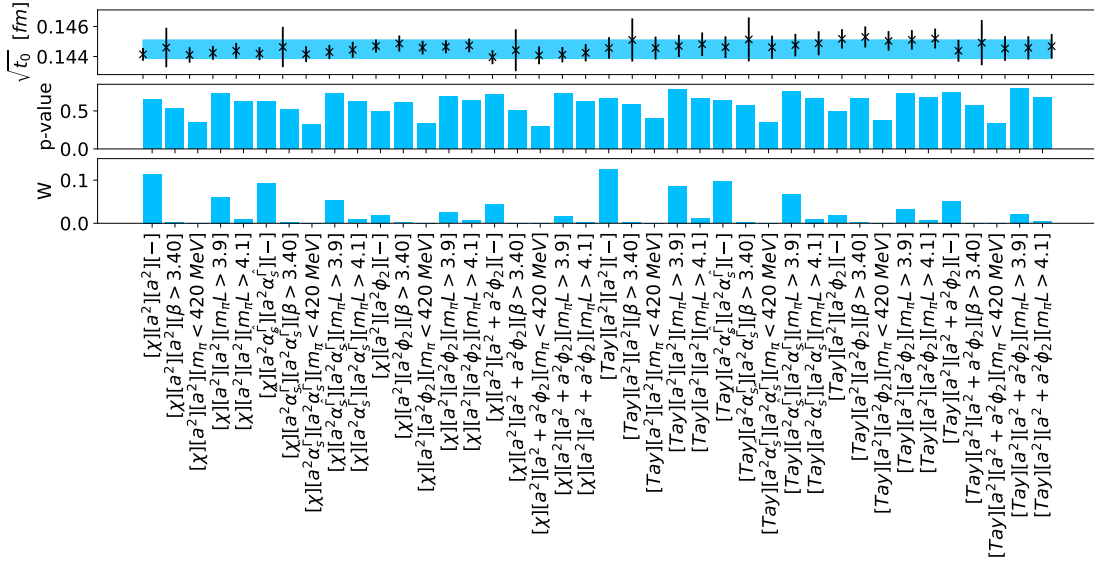


**Figure 3:** Results for  $\sqrt{t_0^{\text{ph}}}$  for the *Combined* data set and for each model considered. The p-value and  $\langle \chi^2 \rangle$  are computed following [19]. The blue band represents the model average following [17] where the systematic error contribution from the model variation has been included. The horizontal axis refers to the considered models: the first tag ( $[X]$  or  $[Tay]$ ) refers to the continuum parameterisation according to eq. (12) or eq. (13), respectively; the second and third tags label the cutoff effects of the Wilson and Wtm subsets of data, respectively ( $[a^2]$  if only  $c_1$  in eq. (14) is switched on,  $[a^2\alpha_s^{\hat{r}}]$  if only  $c_3$  is used,  $[\phi_2 a^2]$  if  $c_2$  is used, or  $[a^2 + \phi_2 a^2]$  if both  $c_1$  and  $c_2$  are considered); and the fourth tag corresponds to the cuts performed in both Wilson and Wtm data for the fit ( $[\beta > 3.40]$  if only ensembles with  $\beta > 3.40$  are kept or  $[m_\pi < 420 \text{ MeV}]$  if symmetric point ensembles are discarded). Although only a subset of the models do have a significant weight, we observe that the error band from the model averaging covers the results of all the individual models. The first model in the x-axis corresponds to the one illustrated in Fig. 2.

MCIN/AEI/10.13039/501100011033 and by “ERDF A way of making Europe”, and by the Spanish Research Agency (Agencia Estatal de Investigación) through grants IFT Centro de Excelencia Severo Ochoa SEV-2016-0597 and No CEX2020-001007-S, funded by MCIN/AEI/10.13039/501100011033. We also acknowledge support from the project H2020-MSCAITN-2018-813942 (EuroPLEx), under grant agreement No. 813942, and the EU Horizon 2020 research and innovation programme, STRONG-2020 project, under grant agreement No 824093.

## References

- [1] G. Herdoíza, C. Pena, D. Preti, J. Á. Romero and J. Ugarrio, “A tmQCD mixed-action approach to flavour physics”, EPJ Web Conf. 175 (2018), 13018, [arXiv:1711.06017 [hep-lat]].
- [2] A. Bussone et al. [ALPHA], “Heavy-quark physics with a tmQCD valence action”, PoS LATTICE2018 (2019), 270, [arXiv:1812.01474 [hep-lat]].
- [3] J. Ugarrio et al. [Alpha], “First results for charm physics with a tmQCD valence action”, PoS LATTICE2018 (2018), 271, [arXiv:1812.05458 [hep-lat]].

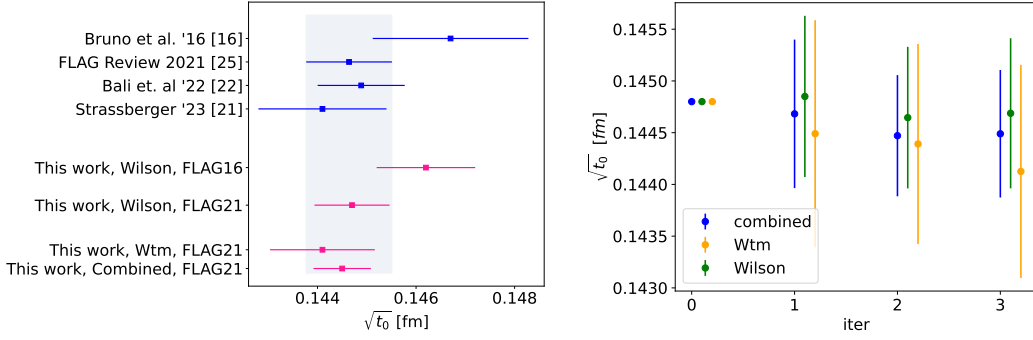


**Figure 4:** Left: Results for the gradient flow scale  $\sqrt{t_0}$  in physical units based on the model average (pink points) for our three types of analysis (Wilson, Wtm and Combined), compared with the  $N_f = 2 + 1$  FLAG average [25] and with other determinations also based on  $N_f = 2 + 1$  CLS ensembles (blue points). Since in Bruno et al. [16] the FLAG16 [24] prescription was used to set in the physical input, we also show the result of our analysis using the Wilson regularisation with FLAG16 physical input ("This work, Wilson, FLAG16") instead of FLAG21 [25] ("This work, Wilson, FLAG21"). The CLS results, Bali et al. [22] and Strassberger [21], use FLAG21 [25] physical input. Right: results of  $\sqrt{t_0}$  for the three types of analysis at each iteration of the scale setting analysis. The initial iteration starts from a  $t_0$  value without error and the  $i$ -th iteration starts with the value of  $t_0^{\text{ph}}$  of the  $(i - 1)$ -th iteration. After four iterations of the scale setting analysis we observe signs of convergence for the value of  $t_0$ .

- [4] A. Bussone et al. [ALPHA], "Matching of  $N_f = 2 + 1$  CLS ensembles to a tmQCD valence sector", PoS LATTICE2018 (2019), 318, [arXiv:1903.00286 [hep-lat]].
- [5] J. Frison et al., "Heavy semileptonics with a fully relativistic mixed action", PoS LATTICE2019 (2019), 234, [arXiv:1911.02412 [hep-lat]].
- [6] G. Herdoiza et al., PoS LATTICE2022 (2022), 268.
- [7] A. Bussone, A. Conigli, J. Frison, G. Herdoiza, C. Pena, D. Preti, A. Saez, J. Ugarrío, "Hadronic physics from a Wilson fermion mixed-action approach: Charm quark mass and  $D_{(s)}$  meson decay constants", [arXiv:2309.14154].
- [8] A. Conigli et al., PoS LATTICE2022 (2022), 235.
- [9] J. Frison et al., PoS LATTICE2022 (2022), 378.
- [10] M. Lüscher and S. Schaefer, "Lattice QCD without topology barriers", JHEP 07 (2011), 036, [arXiv:1105.4749 [hep-lat]].
- [11] M. Bruno et al., "Simulation of QCD with  $N_f = 2 + 1$  flavors of non-perturbatively improved Wilson fermions", JHEP 02 (2015), 043, [arXiv:1411.3982 [hep-lat]].
- [12] R. Frezzotti and G. C. Rossi, JHEP 08 (2004), 007, doi:10.1088/1126-6708/2004/08/007, [arXiv:hep-lat/0306014 [hep-lat]].
- [13] R. Frezzotti et al. [Alpha], "Lattice QCD with a chirally twisted mass term", JHEP 08 (2001), 058, [arXiv:hep-lat/0101001 [hep-lat]].
- [14] C. Pena, S. Sint and A. Vladikas, "Twisted mass QCD and lattice approaches to the Delta I=1/2 rule", JHEP 09 (2004), 069, [arXiv:hep-lat/0405028 [hep-lat]].
- [15] D. Mohler, S. Schaefer and J. Simeth, "CLS 2+1 flavor simulations at physical light- and strange-quark masses", EPJ Web Conf. 175 (2018) 02010, [1712.04884].

- [16] M. Bruno, T. Korzec and S. Schaefer, “Setting the scale for the CLS 2 + 1 flavor ensembles,” *Phys. Rev. D* **95** (2017) no.7, 074504, doi:10.1103/PhysRevD.95.074504, [arXiv:1608.08900 [hep-lat]].
- [17] William I. Jay and Ethan T. Neil, “Bayesian model averaging for analysis of lattice field theory results”, *Phys. Rev. D* **103**, 114502 (2021), doi:10.1103/PhysRevD.103.114502, [arXiv:2008.01069].
- [18] J. Frison, “Towards fully bayesian analyses in Lattice QCD”, [arXiv:2302.06550].
- [19] Mattia Bruno and Rainer Sommer, “On fits to correlated and auto-correlated data”, [arXiv:2209.14188].
- [20] Jochen Heitger, Fabian Joswig, Simon Kuberski, “Determination of the charm quark mass in lattice QCD with 2+1 flavours on fine lattices”, *JHEP* 2021, 288 (2021), [arXiv:2101.02694].
- [21] B. Straßberger, “Towards Higher Precision Lattice QCD Results: Improved Scale Setting and Domain Decomposition Solvers,” doi:10.18452/26517
- [22] G. S. Bali *et al.* [RQCD], “Scale setting and the light baryon spectrum in  $N_f = 2 + 1$  QCD with Wilson fermions,” *JHEP* **05** (2023), 035 doi:10.1007/JHEP05(2023)035 [arXiv:2211.03744 [hep-lat]].
- [23] Gilberto Colangelo and Stephan Durr and Christoph Haefeli, “Finite volume effects for meson masses and decay constants”, [arXiv:hep-lat/0503014].
- [24] S. Aoki *et. al.*, “Review of lattice results concerning low-energy particle physics”, [arXiv:1607.00299].
- [25] Y. Aoki *et. al.*, “FLAG Review 2021”, *Eur.Phys.J.C* 82 (2022) 10, 869, doi:10.1140/epjc/s10052-022-10536-1, [arXiv:hep-lat/2111.09849].
- [26] Nikolai Husung, “Logarithmic corrections to  $O(a)$  and  $O(a^2)$  effects in lattice QCD with Wilson or Ginsparg-Wilson quarks”, [arXiv:hep-lat/2206.03536].
- [27] A. Saez, A. Conigli, J. Frison, G. Herdoíza, C. Pena and J. Ugarrio, *PoS LATTICE2022* (2023), 357 doi:10.22323/1.430.0357